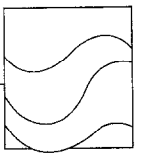

Air–sea CO_2 fluxes in a coastal embayment affected by upwelling: physical versus biological control

Marta ÁLVAREZ[a*], Emilio FERNÁNDEZ[b], Fiz F. PÉREZ[a]

[a] Instituto de Investigaciones Marinas (CSIC), C/ Eduardo Cabello N° 6, 36208, Vigo, Spain
[b] Facultad de Ciencias, Universidad de Vigo, Campus Lagoas-Marcosende, 36200, Vigo, Spain

(Received 2 April 1998, revised 11 March 1999, accepted 28 April 1999)

Abstract – Water column pCO_2 and air–sea CO_2 fluxes were studied during an 18-month period (May 1994–September 1995) in a coastal embayment affected by upwelling, located in the northwestern Iberian Peninsula (Ria de Vigo and adjacent shelf). Overall, the region acted as a net annual atmospheric CO_2 sink, with magnitude ranging from 0.54 mgC m^{-2} d^{-1} in the Ria estuary to 22 mgC m^{-2} d^{-1} offshore. During moderate upwelling and upwelling relaxation conditions the sampling area was a sink for atmospheric CO_2. By contrast, during winter conditions and during intense upwelling the flux reversed towards the atmosphere. The relative influence of physical and biological processes on pCO_2 was evaluated using two different approaches: firstly, statistical analysis of physico-chemical correlations, and secondly, a thermodynamic analysis in the oceanic CO_2 system. Both methods yielded consistent results, showing that the main processes controlling seasonal and spatial pCO_2 variability were the production and remineralization of organic matter, explaining ca. 70 % of the total variability. In the inner part of the embayment, air–sea CO_2 exchange was mainly modulated by CO_2 partial pressure gradient, whereas in the adjacent shelf, wind speed largely contributed to CO_2 fluxes between the ocean and the atmosphere. © 1999 Ifremer / CNRS / IRD / Éditions scientifiques et médicales Elsevier SAS

carbon dioxide / air–sea exchange / spatial-temporal variability / physical-biological control / northwestern Iberian Peninsula

Résumé – Échanges air–océan de CO_2 dans une baie côtière affectée par l'*upwelling* : contrôle physique et biologique. Le pCO_2 dans la colonne d'eau et les échanges de CO_2 entre l'air et l'eau ont été étudiés durant 18 mois (mai 1994–septembre 1995) dans une baie affectée par l'*upwelling* au nord-ouest de la péninsule Ibérique (Ria de Vigo et plateau continental adjacent). En moyenne annuelle, cette région est un puits de CO_2 atmosphérique, le flux net air–mer variant de 0,54 à 22 mgC m^{-2} j^{-1}. Durant les périodes d'*upwelling* modéré ou de relaxation de l'*upwelling*, la zone étudiée se comporte comme un puits de CO_2 ; en revanche, durant l'hiver et lors d'événements advectifs forts, cette zone devient une source de CO_2 pour l'atmosphère. L'influence relative des processus physiques et biologiques a été évaluée par deux approches différentes : une analyse statistique et une analyse physico-chimique à partir des relations thermodynamiques. Ces deux méthodes conduisent à des résultats comparables et montrent que les processus principaux qui contrôlent la variabilité spatiale et saisonnière du pCO_2 sont la production et la reminéralisation de la matière organique, qui expliquent 70 % de la variabilité totale. À l'intérieur de la baie, les échanges air–mer de CO_2 sont principalement modulés par le gradient de pression partielle de CO_2, tandis que sur le plateau continental, ils le sont par le coefficient d'échange. © 1999 Ifremer / CNRS / IRD / Éditions scientifiques et médicales Elsevier SAS

dioxyde de carbone / échange air–mer / variabilité spatiale-temporelle / contrôle physique-biologique / nord-ouest de la péninsule Ibérique

* Correspondence and reprints: malvarez@iim.csic.es

1. INTRODUCTION

The relative importance of physical and biological processes in governing surface ocean pCO_2 is still a controversial issue in oceanography [7, 48, 52, 55]. Fixation of dissolved CO_2 by marine phytoplankton leads to a concurrent decrease in total inorganic carbon and pCO_2, whilst pH increases and alkalinity suffers small changes. On the other hand, calcium carbonate production by ocean calcifying organisms changes both alkalinity and total inorganic carbon, however it can lead to an increase in surface pCO_2. Physical processes such as the precipitation/evaporation budget, vertical entrainment and diffusion and horizontal advection and mixing can also control the CO_2 species distribution in the ocean. The preponderance of physico-chemical over biological conditions [7, 53, 64] or vice versa [13, 21, 56, 62] varies spatially and seasonally, being therefore dependent on the regions and seasons considered. However, separating and quantifying the contribution of these various processes was attempted by different authors [4, 6, 14, 25].

Coastal areas represent 8 % of the global oceanic area, and account for about 25 % of marine primary production [59, 65]. These areas are considered as organic carbon deposition and preservation zones and/or shelf-to-ocean exportation areas [59, 61, 65]. In this connection, 3–8 % of the annual atmospheric CO_2 concentration increase is estimated to be buried as organic carbon in coastal marine environments [31]. However, the contribution of these areas is usually underestimated in global carbon models [11, 65].

This study was carried out in a coastal and estuarine area of the northwestern Iberian Peninsula (Ria of Vigo, *figure 1*) with the general aim of gaining understanding on the air–sea CO_2 flux in a coastal region affected by wind-driven upwelling [10, 18]. The Ria of Vigo is a coastal embayment in the western coast of Galicia (NW Spain) defined as a positive estuary, with the following pattern of inner positive circulation: the river discharge flows outwards at the surface balanced by a net inward flow at the lower levels [19]. The inner circulation and water exchange with the shelf are both affected by wind-driven upwelling which is common along the eastern boundary of the North Atlantic between 10° and 44° N [66]. Northerly winds cause upwelling of salty, cold North Atlantic Deep Water (NADW) from April to October, although mainly in summer [18, 36]. By contrast, southerly winds prevail from November to March generating downwelling. During strong downwelling events water circulation can be reversed, and so oceanic coastal water flows into the Ria [1, 10, 16].

River discharge contributes to maintaining the inner positive circulation within the Ria and the water column sta-

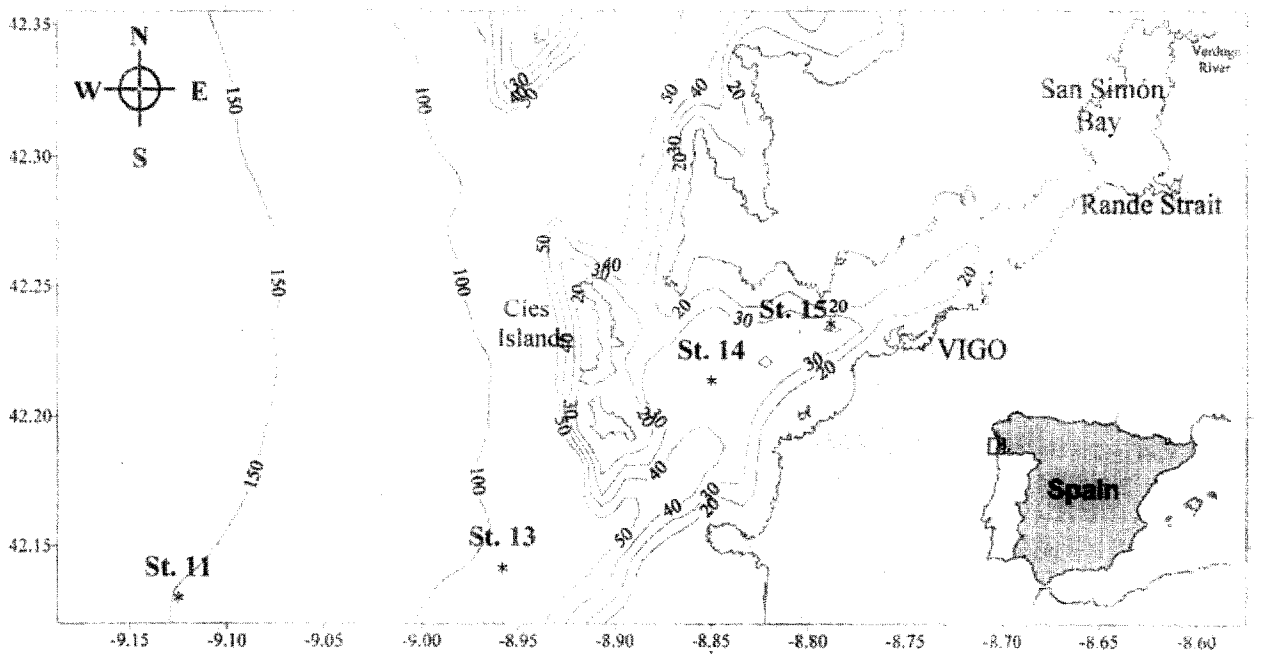

Figure 1. Map of the sampled stations.

bility, which determines water column resistance against the deforming effects of wind [1]. The main tributary to the Ria of Vigo is the Verdugo River with an average run-off of 13.2 $m^3 s^{-1}$ [46]. This river is characterized by very low alkalinity and calcium levels, which behave conservatively during estuarine mixing, and also by low levels of nutrient salts, which from late spring to autumn are mainly determined by biological activity of the estuarine and benthic biota at the innermost part of the Ria (San Simón Bay) [37].

Besides the general aim already outlined, four main objectives were formulated in this investigation: i) to study the seasonal variability of the water column pCO_2, ii) to analyse the estuarine–shelf gradient in pCO_2, iii) to evaluate the influence of physical, chemical and biological factors on water column pCO_2 variability, iv) to quantify air–sea CO_2 fluxes in this area throughout a seasonal cycle.

2. MATERIAL AND METHODS

Four stations located along the central axis of the Ria of Vigo were sampled fortnightly from May 1994 to September 1995 (*figure 1*). However, due to bad weather conditions in winter some samplings were missed, especially at station 11. Hereinafter both external stations considered are located at the shelf, stations 11 and 13, and internal stations are those located inside the Ria, stations 14 and 15.

Temperature, salinity and pressure were obtained with a SBE25 CTD probe. Salinity and density were calculated using the equations of Unesco [57]. The upwelling index (Iw) was calculated at 43° N 11° W (150 km off Cape Finisterre) following Bakun [5], using geostrophic winds derived from surface pressure charts (three times per day). The vectors were multiplied by 0.7 and cyclonically rotated 15° to estimate surface wind velocity. Negative values of Iw indicate downwelling.

The flow of fresh water to the Ria of Vigo (Qr, in $m^3 s^{-1}$) was calculated as in Ríos et al. [46] using the drainage area and rainfall data.

Water samples were taken with 5-L Niskin bottles from three to eight depths (depending on the bathymetry) to determine nutrients (ammonium, nitrate and nitrite), dissolved oxygen and chlorophyll *a* concentrations as well as alkalinity and pH.

Dissolved oxygen (µmol kg^{-1}) was measured using Winkler potentiometric titration, and chlorophyll *a* (Chl *a*) was determined fluorometrically after extraction with 90 % acetone overnight.

pH was measured with a combined glass electrode standardised with NBS buffer solutions of 7.413 and 4.008 pH. The electrode was then adapted to seawater ionic strength in natural seawater CO_2 free borax 4.4 pH buffer solution. Temperature was measured using a platinum resistance thermometer and pH was finally referred to 15 °C (pH_{15}) according to Pérez and Fraga [38]. The accuracy of the analytical procedure used in this investigation was ± 0.005 pH units.

Alkalinity was determined by potentiometric titration with HCl to a final pH of 4.44 according to Pérez and Fraga [39], using a Metrohm E-410 pH-meter with a separated glass electrode and a reference electrode connected to an automatic burette and an impulsomat. The electrode was standardised with NBS buffer solutions of 7.413 and 4.008 pH. This method displayed an accuracy of ± 2 µmol kg^{-1}. On every station, alkalinity samples were taken from surface, intermediate and bottom waters.

Total inorganic carbon (TIC) and partial pressure of CO_2 (pCO_2) were estimated from pH_{15} and alkalinity data using thermodynamic equations of the carbonate system [15] and the constants determined by Mehrbach et al. [33] and Weiss [63] with an accuracy of ± 4 µmol kg^{-1} and ± 8 µatm, respectively [27, 34]. We used Mehrbach constants rather than more recent constants [50] since the temperature effect on pCO_2 obtained using Mehrbach constants is more consistent with the experimental values [27, 35, 54]. In order to verify this procedure, a comparative experiment was performed between 3 January and 27 March 1994 in the South Atlantic where pCO_2 was determined directly and also calculated from pH_{15} and alkalinity using the above procedure [12, 47]. The results were very similar with an average and standard deviation of 1 ± 7 µatm [45].

The CO_2 air–sea exchange (mg $m^{-2} d^{-1}$) was calculated using the following equation:

$$F = 2.88 . k \ S . (pCO_2oc - pCO_2at)$$

where k is the piston or transfer velocity (cm h^{-1}), S is CO_2 seawater solubility (mol kg^{-1} atm^{-1}), pCO_2oc is surface ocean CO_2 partial pressure, pCO_2at is atmospheric CO_2 partial pressure (both in µatm) and 2.88 is a conversion factor.

Seasonal and inter-annual variations in the atmospheric pCO_2 are small when compared to pCO_2 variations in the

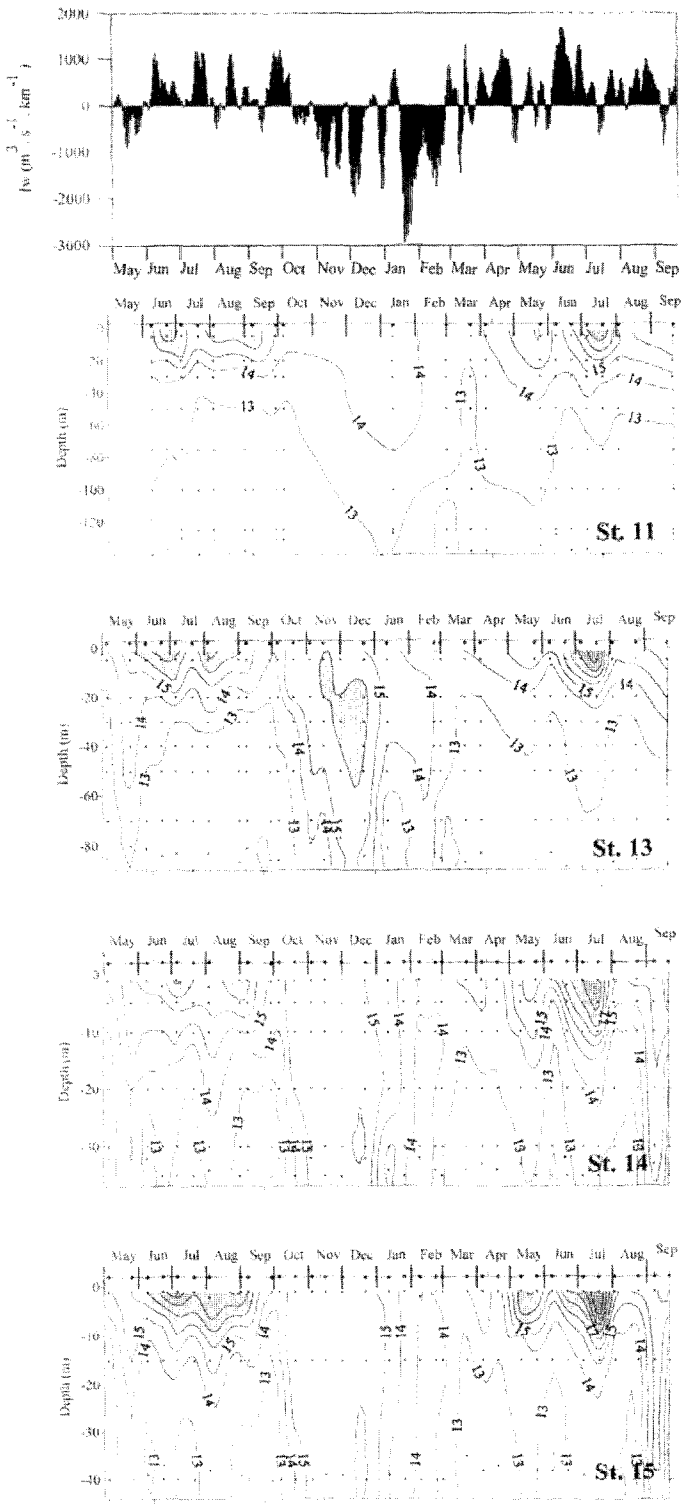

Figure 2. Temporal variability of upwelling index (Iw) and temperature (°C) at the sampling stations. Points over the top axis represent sampling dates.

ocean surface [3]. On the other hand, Keeling and Whorf [24] have reported the annual atmospheric molar fraction of CO_2 (xCO_2) at Mauna Loa Station, which were linearized by Pérez et al. [40] according to the following equation:

$$xCO_2at\ (ppm) = 279 + e^{0.134 \cdot (y - 1850)^{0.7}}$$

where y is the year. The lack of pCO_2at data led us to use a constant pCO_2at calculated as the mean pCO_2at value of the two considered years (1994 and 1995) using the previous equation and assuming a mean atmospheric pressure of 1 atm. Thus, pCO_2at was assumed to be 357 µatm.

The piston velocity, k, was calculated using the equations derived from those suggested by Liss and Mervilat [29] and proposed by Woolf and Thorpe [67], the former are more suitable given that the range of temperature in our data lies between 13 and 21 °C:

$$k = 0.17\ U_{10}\ (600/Sc)^{2/3}$$

$U_{10} < U_1$ for smooth water regime.

$$k = (2.85\ U_{10} - 9.65)\ (600/Sc)^{1/2}$$

$U_{10} > U_1$ for rough water regime.

$$U_1 = 9.65\ (2.85 - 0.17\ (600/Sc)^{1/6})^{-1}$$

where Sc is the Schmidt number (the ratio of the cinematic viscosity of the water to the molecular diffusivity of the gas), and U_{10} is wind speed 10 m above the sea level (m s^{-1}). The Schmidt number was calculated from its relation with temperature derived from data tabulated by Andrié et al. [3] obtained by Ríos et al. [44]:

$$\ln (600/Sc) = -1.0687 + 0.05127\ T \quad r^2 = 0.995$$

where Sc is the Schmidt number and T is temperature (°C). Seawater CO_2 solubility was deduced from Weiss [63].

Wind speed data were obtained from two meteorological stations, located at Cape Finisterre (43° N, 11° W) and in the Ria of Vigo (42° 14'N, 8° 48' W). Raw wind speed data were averaged daily. Wind speed data corresponding to the date of the survey as well as the dates previous and posterior were squarely averaged to obtain the mean wind speed used for the calculation of the exchange coefficient equation. A shelf-Ria linear gradient (i.e. a linear gradient between the wind speed data from the Finisterre and the Ria of Vigo databases) was assumed during each survey. The estimated mean slope of this gradient was very similar to that obtained from wind speed data collected in the same area during a series of cruises carried out from June to December 1997.

3. RESULTS

3.1. Thermohaline characteristics

Figure 2 shows the temporal variability of the upwelling index and of temperature for the different stations. The temporal variability of fresh water flow and salinity are shown in *figure 3*. Vertical displacements of the 13 °C isotherm (*figure 2*), which defined approximately the upper limit of upwelled water in this area [16], are correlated with the displacements of the upwelling index, Iw, calculated from geostrophic winds. However, it is necessary to take into account that the inertia of coastal circulation to wind stress is about three days and the relaxation is even slower [32]. Therefore, the relationship between Iw and the vertical displacements of the 13 °C isotherm is not so straightforward. However, four hydrographic situations can nevertheless be discerned throughout the seasonal cycle:

Winter conditions dominated from October 1994 through to February 1995 and were characterized by thermal and haline homogeneity of the water column due to strong vertical mixing. However several phenomena occurred in between. Thermal inversions maintained by the haline gradient were detected in stations 13, 14 and 15 during December 1995 (*figure 2*). During this period Iw was, as a mean, highly negative, leading to a flow towards the Ria of surface oceanic water saltier (35.7–35.8) and warmer (15–16 °C) than that flowing out of the Ria (14–15 °C and 34.2–34.6) (*figures 2, 3*). As the latter had a lower density it invaded the water column, giving rise to the thermal inversions detected in December 1995. In January 1995, a sharp change in wind regime caused an upwelling pulse of NADW, which was, however, retained at deep layers due to the restoring of previous conditions. In later January and in February–March 1995 the water column was almost totally occupied by low salinity water at the inner stations due to high continental runoff (St. 14 and 15, *figure 3*) while at the external ones (St. 11 and 13, *figure 3*) cold and saltier water was detected. From March 1995 onwards, spring–summer conditions were established and upwelling/relaxation pulses succeed.

Moderate upwelling. Upwelled water, defined by the 13 °C isotherm, did not reach the surface layer (top 20 m), thus enabling thermal and haline gradients to develop, especially at the internal stations (14 and 15). June, late August and early September 1994 and March and early April 1995 were typical periods of this condition (*figures 2, 3*). The limit between moderate and

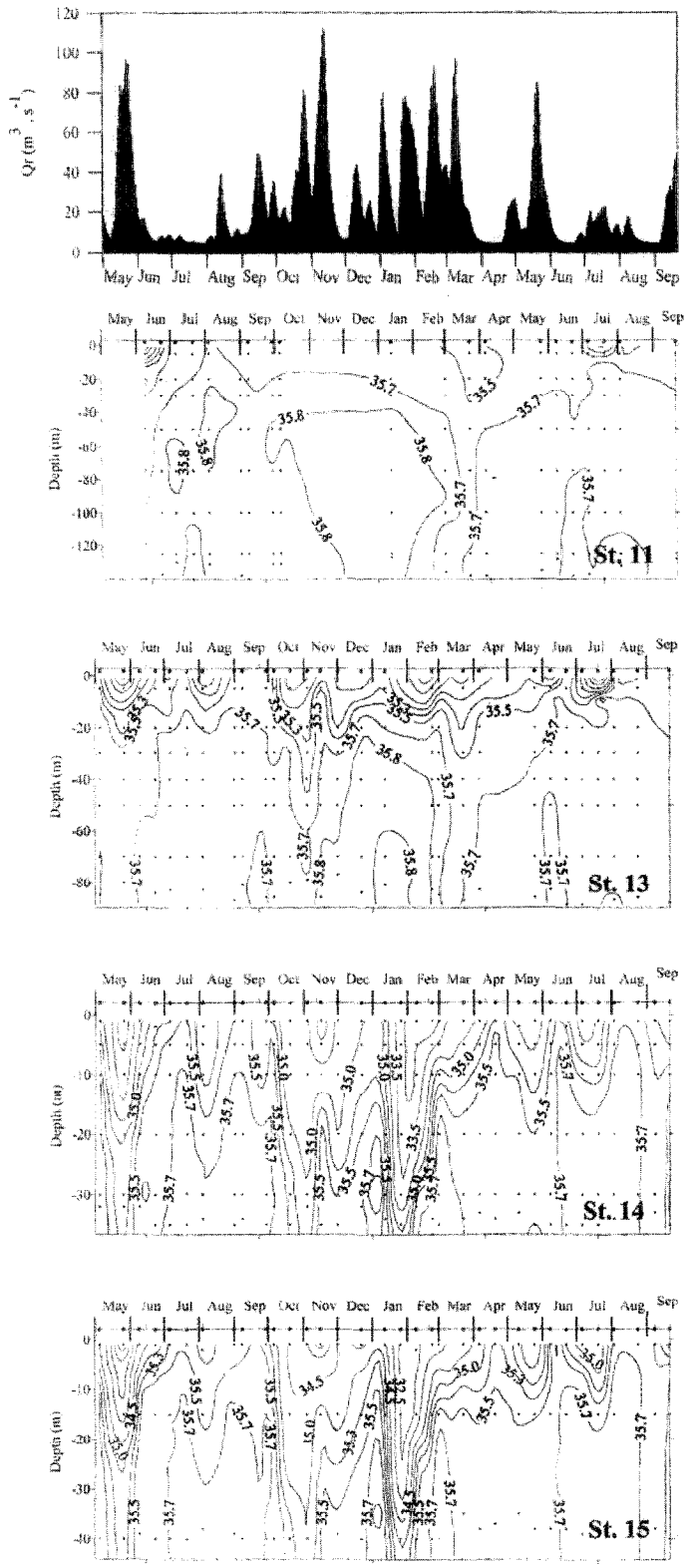

Figure 3. Temporal variability of fresh water flow (Qr) and salinity at the sampling stations. Points over the top axis represent sampling date

intense upwelling conditions was established at Iw values of 1000 $m^3 s^{-1} km^{-1}$.

Intense upwelling. Temperature decreased in the whole water column, whereas salinity increased and the thermocline was eroded, thus subsurface waters reached the surface layer. This situation took place in July and September 1994 and early June, and August 1995 (*figures 2, 3*) at all the sampled stations. Generally, moderate and intense upwellings are intensified in the inner part of the Ria due to topographic interactions, upwelled water reaches higher levels than in the more external

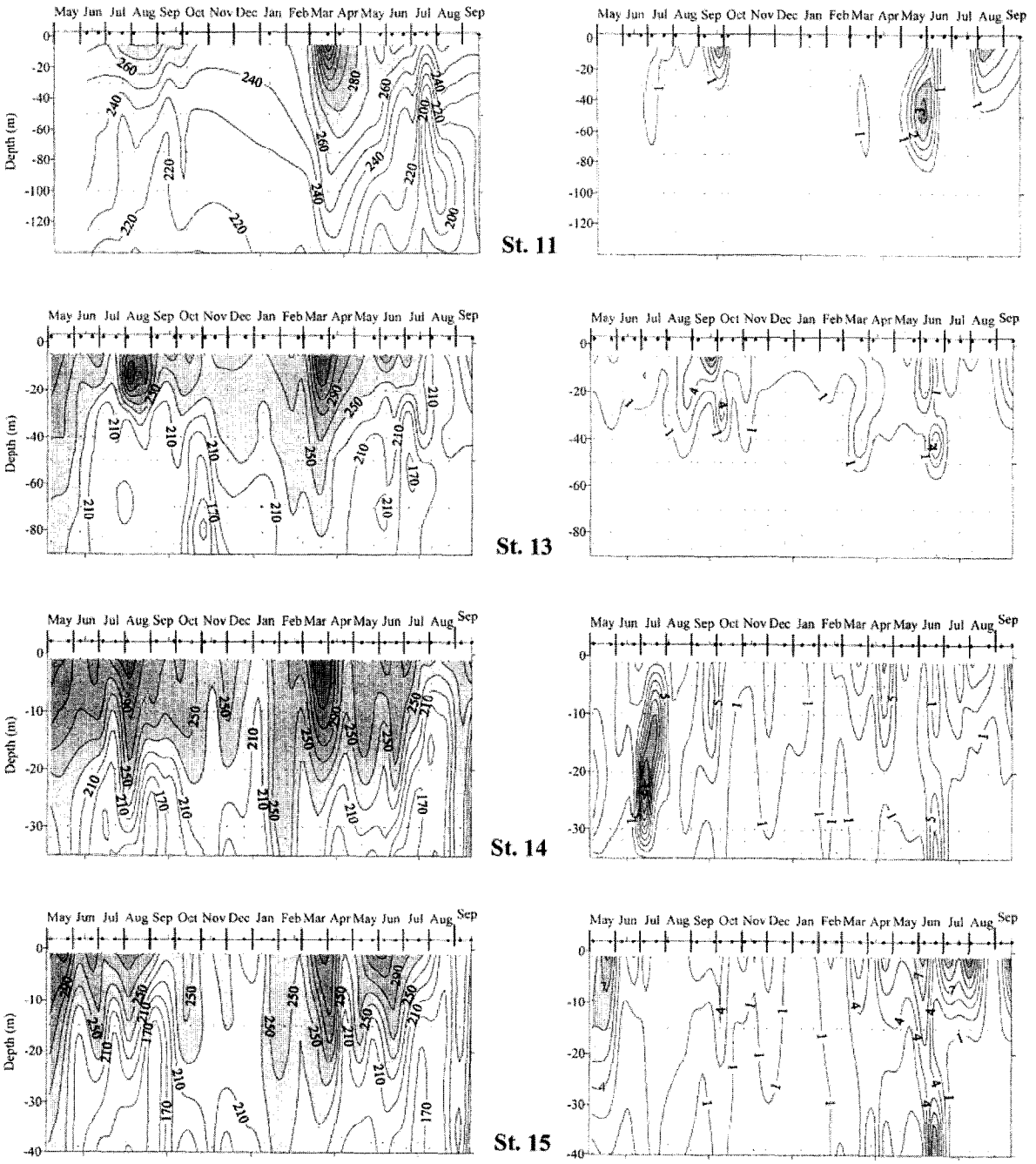

Figure 4. Temporal variability of dissolved oxygen (µmol kg^{-1}) and chlorophyll *a* (mg m^{-3}) concentrations at the sampling stations. Points over the top axis represent sampling dates.

zones. In this sense, the isotherm of 13 °C was detected during late September 1994 at about 15 m depth at station 15 and at about 25 m at station 13.

Upwelling relaxation. Iw decreased in parallel to a reduction in the strength of northerly winds. Surface circulation of less saline water flowing from the inner part of the Ria into the ocean is slowed down, and strong haline and thermal surface gradients developed due to reduced advection. May, early August 1994 and April, May, late June, July and September 1995 were examples of these conditions (*figures 2, 3*).

3.2. Chlorophyll *a* and dissolved oxygen concentrations

High chlorophyll *a* concentrations (*figure 4*) were associated with upper layer stability and a shallow nutricline [16]. These conditions were achieved during periods of moderate upwelling and after the first pulse of intense upwelling when photosynthetic organisms begin to develop as a response to favourable irradiance and nutrient conditions, as in the inner stations during June 1994 where Chl *a* concentrations from 3 to 4 mg m^{-3} were measured. Subsurface chlorophyll maxima were usually related to relaxation periods such as at the end of June 1995 in stations 13, 14 and 15. During these periods phytoplankton accumulated in the upper layer after an upwelling event due to the reduced 'washout' compared to their doubling times [1, 49]. On the other hand, a high subsurface chlorophyll maximum (17 mg m^{-3}) at station 14 during early July 1994 was associated with an intense upwelling period. Variations in the upwelling index shown in *figure 2* indicate that this survey was performed during a spin up period of the upwelling pulse, when the motion pattern of subsurface water advects sinking phytoplankton cells up to the surface [1]. In winter (from November 1994 until February 1995) chlorophyll *a* concentration was low (0.5–3 mg m^{-3}) throughout the water column.

Inner stations showed a high variability of dissolved oxygen concentration (*figure 4*), with values higher than 260 µmol kg^{-1} in the surface layer in spring and summer when enhanced photosynthetic activity was expected to occur. In March and April 1995, the spring phytoplankton bloom took place and oxygen values were higher than 310 µmol kg^{-1} (*figure 4*, station 14, and 360 µmol kg^{-1} oxygen maxima). The same situation was observed at offshore stations with values of around 300–340 µmol kg^{-1}. In winter and during intense upwelling, when low-oxygen water bodies reached the surface layer, the 260 µmol kg^{-1} oxygen isoline generally disappeared. By contrast, during upwelling relaxations, oxygen concentrations in the whole water column rose due to the displacement of surface oxygen-rich waters to lower levels. Subsurface oxygen minima remained at the inner stations during late August 1995 and early September 1995 due to advection of upwelled water aged on the shelf [16]. At the external stations subsurface oxygen minima were identified in early November 1994 during winter conditions, and late June 1995 corresponding to a period of upwelling.

3.3. pCO_2

The temporal variability of seawater pCO_2 is shown in *figure 5*, where the 357 µatm isoline representing the mean atmospheric pCO_2 for the studied period is emphasized. The Ria of Vigo and adjacent shelf regions were sinks for atmospheric CO_2 during most of the studied period except in winter (November 1994 to February 1995) and during some intense upwelling events (station 13 July 1994, station14 and 15 September 1994 and at stations 13, 14 and 15 in August 1995) when the flux reversed, and seawater was a source of CO_2 to the atmosphere. Surface pCO_2 minima in May 1994 (220–260 µatm), August 1994 (260–300 µatm) and March–April 1995 (220–280 µatm) corresponded with oxygen maxima at the surface.

Subsurface pCO_2 variability was influenced by upwelling/relaxation dynamics. Relaxations tended to decrease water column pCO_2 while upwellings bring high pCO_2 waters to the surface. In winter, pCO_2 was high (380–500 µatm). A clear relationship was found between subsurface pCO_2 maxima (500–600 µatm) and the previously commented oxygen subsurface minima.

3.4. pCO_2 variability: physical vs. biological control

With the aim of isolating the factors controlling the temporal variation of pCO_2, two sets of analysis were performed. Firstly, a statistical analysis was undertaken revealing the relationship between pCO_2 and physical (temperature and salinity), chemical and biological (chlorophyll *a* and oxygen concentrations) variables. Secondly, an analysis based on the thermodynamic relationships between pCO_2 and physico-chemical variables defining the seawater CO_2 system.

1) *Figure 6* shows the relationship observed between pCO_2 and temperature, salinity, Chl *a* and dissolved oxygen concentration. A statistically significant linear relationship was observed between pCO_2 and dissolved oxygen concentration when considering both surface and

water-column data. By contrast, pCO_2 and temperature, salinity or Chl *a* were not significantly related. Chl *a* is affected by sedimentation and grazing processes, thus it is not considered a conservative parameter. On the other hand, pCO_2 and oxygen have a more conservative behaviour than Chl *a*, therefore despite the lack of correlation between pCO_2 and Chl *a*, the relationship between pCO_2 and oxygen points to biological activity as the main process controlling pCO_2 distribution and, indirectly, air–sea CO_2 fluxes.

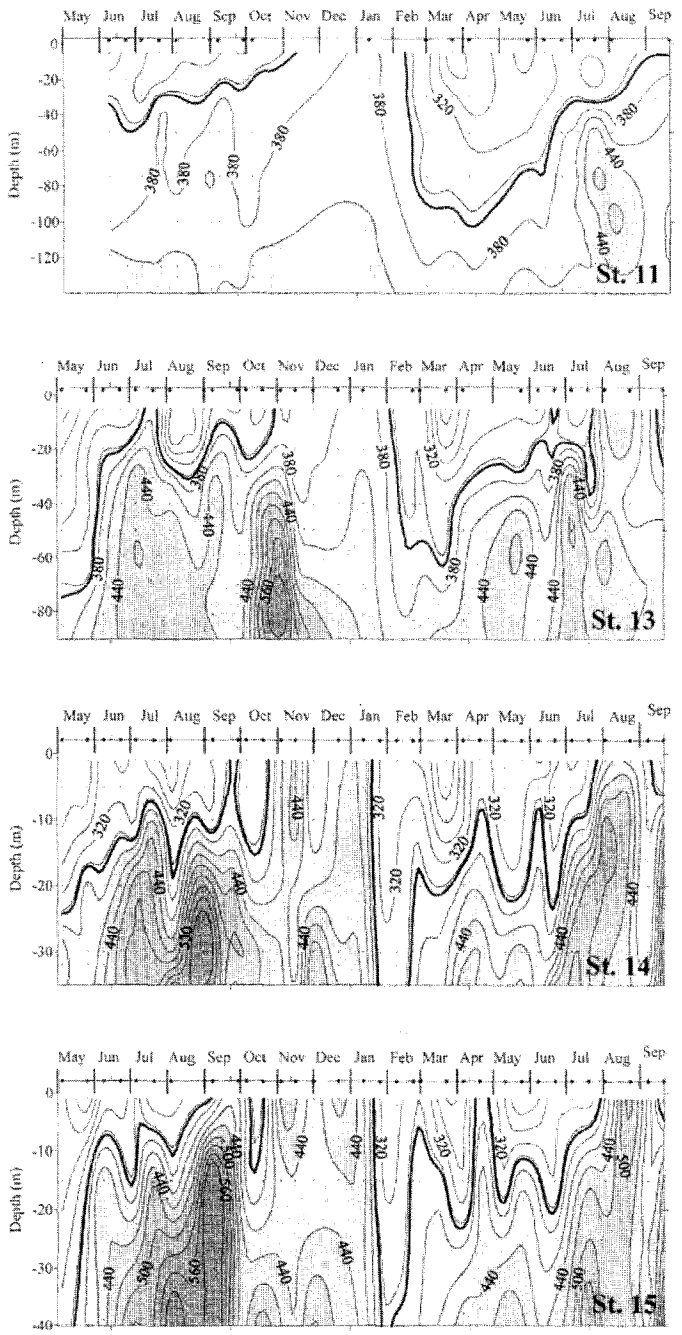

Figure 5. Temporal variability of calculated pCO_2 (µatm) at the sampling stations. Points over the top axis represent sampling dates. The emphasized isoline represents the mean atmospheric pCO_2 during the sampling period (357 µatm).

2) In order to evaluate the magnitude of the different processes affecting pCO_2 in our study area we followed the methodology proposed by Sabine and Key [51]. Neglecting water mass mixing, pCO_2 for any water sample can be generated by correcting for temperature change, dilution, organic matter and carbonate production / remineralization. In this case, the initial conditions are the mean characteristics of the upwelled water during the sampled period (*table I*). It was assumed that the water present in the Ria is a mixture of subsurface upwelled water and

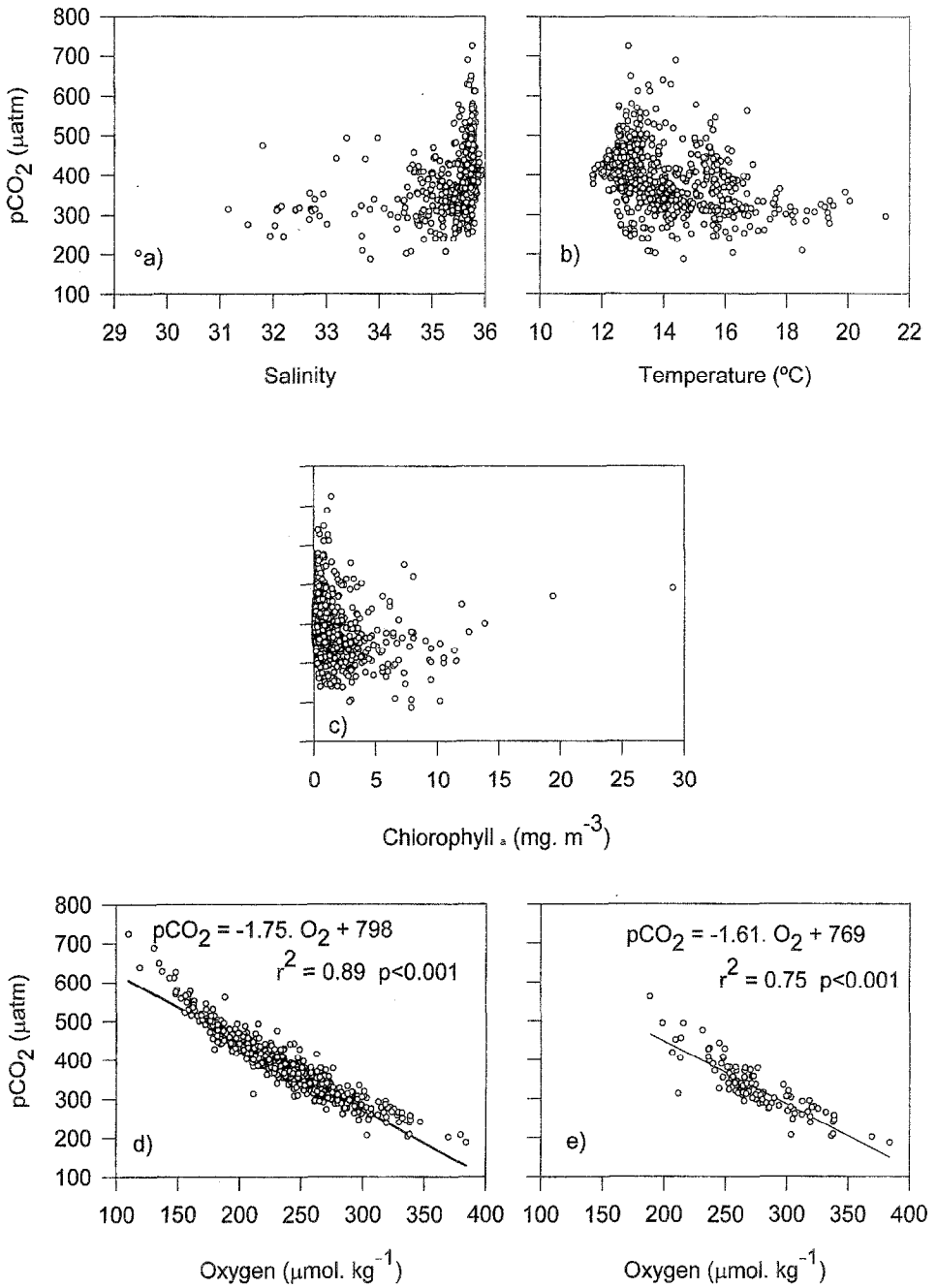

Figure 6. Relationships between pCO_2 (µatm) and water column (a) salinity, (b) temperature, (c) chlorophyll *a*, (d) dissolved oxygen concentrations and (e) dissolved oxygen concentration at the surface layer.

water derived from continental runoff. pCO_2 for any sample was predicted from the initial conditions (*table I*) by correcting the previously enumerated effects on the mean pCO_2 of upwelled water. The variability not accounted for by this model can be attributed to the presence of additional water masses and/or air–sea exchange.

Table I. Initial conditions for the upwelled water in the Ria.

Parameter	Symbol	Value
Salinity	S^0	35.71
Temperature (°C)	T^0	12.34
Alkalinity (µmol/kg)	$Alk.^0$	2345
TIC (µmol/kg)	TIC^0	2140
pCO_2 (µatm)	pCO_2^0	423
AOU (µmol/kg)	AOU^0	49.8
NO_3 (µmol/kg)	NO_3^0	10.24

Temperature correction. The heat-flux corrected values of pCO_2 (pCO_{2T}) were calculated using the full set of equilibrium equations referred to in the 'Material and methods' section as a function of measured temperature (T), and the initial conditions for salinity, alkalinity and TIC (S^0, Alk^0, TIC^0 respectively, *table I*).

$$pCO_{2\,T} = f(T, S^0, Alk^0, TIC^0).$$

Dilution correction. The addition or removal of water can be estimated from changes in salinity, but it must be taken into account that both Alk. and TIC are also proportionally diluted and that the river also contributes to Alk. and TIC, adding about 105 µmol/kg and 210 µmol/kg, respectively (J. Gago, pers. comm.). For calculating pCO_2 values corrected for heat and water flux ($pCO_{2\,T\,S}$), TIC and Alk. should be also normalized to the initial value of salinity.

$$Alk._S = Alk^0 \cdot S / S^0 + 105 \cdot (1 - S / S^0)$$

$$TIC_S = TIC^0 \cdot S / S^0 + 210 \cdot (1 - S / S^0)$$

$$pCO_{2\,T\,S} = f(T, S, Alk._S, TIC_S).$$

Organic matter correction. Biological activity in the area is estimated from changes in the Apparent Oxygen Utilization (AOU) concentration. The difference between the AOU measured at each point and the reference AOU is proportional to the biological uptake/regeneration using a stoichiometric $-O_2$:C ratio or photosynthesis quotient (PQ), typically between 1.0 and 1.4 for marine organic matter production [26]. In this study we used a PQ = 1.36 according to Ríos et al. [43] for phytoplankton of the Ria of Vigo. This PQ did not differ significantly from those calculated by Anderson [2] and Fraga et al. [20]. TIC is also largely affected by these processes. In the case of alkalinity, Alk_S should be corrected for the uptake of one mole of H+ for every mole of nitrate (N) during photosynthesis [8, 23], but the effect is much lower. Corrected Alk., TIC and pCO_2 for heat and water flux and biological processes were computed as:

$$Alk._{S\,N} = Alk_S + (N^0 - N)$$

$$TIC_{S\,AOU} = TIC_S - (AOU^0 - AOU) / PQ$$

$$pCO_{2\,T\,S\,AOU} = f(T, S, Alk._{S\,N}, TIC_{S\,AOU}).$$

Calcium carbonate correction. Carbonate precipitation/dissolution affects Alk and TIC in a 2:1 ratio. Corrected TIC and pCO_2 for heat and water flux, biological processes and carbonate precipitation/dissolution were computed as:

$$TIC_{S\,AOU\,Ca} = TIC_{S\,AOU} - 0.5 \cdot (Alk._{S\,N} - Alk.)$$

$$pCO_{2\,T\,S\,AOU\,Ca} = f(T, S, Alk., TIC_{S\,AOU\,Ca}).$$

Predicted pCO_2 ($pCO_{2\,T\,S\,AOU\,Ca}$) and that calculated from measured pH_{15} and alkalinity showed a highly significant relationship ($r^2 = 0.88$; $p < 0.0001$ for the whole water column and $r^2 = 0.57$; $p < 0.0001$ considering surface data only).

Table II shows the percentage of pCO_2 variation explained by each process, which was calculated as the ratio between the variance of pCO_2 derived by each one and the total variance of pCO_2. The main conclusion derived from these results is that biological activity was the main process modulating pCO_2 variability in the set of sampled stations. Temperature, dilution and calcium carbonate processes also influenced pCO_2 variability, although to a lower extent considering both surface waters and the whole water column.

The temperature dependence of surface pCO_2 varied around 33 %, except at station 11 where it was as high as 67 %. Dilution processes explained only 0 to 3 % of the surface pCO_2 variability. In the outermost station temperature changes were about ten-fold those of salinity, explaining the high % attributed to thermal flux. Carbonate precipitation/dissolution reactions explained always less than 7 % of the surface pCO_2 changes. These reactions had their greatest influence on the surface pCO_2 variability of station 14.

3.5. Air–sea CO_2 fluxes

Figure 7 shows the spatio-temporal variability in air–sea CO_2 fluxes. The pattern of variability found at the inner stations (stations 14 and 15) differed from that found in the

Table II. Average pCO_2, standard deviation and percentage of pCO_2 variability explained by each process (%), considering surface and water column as a whole. n represents the number of samples.

	St. 11 (n=20)	St. 13 (n=29)	St. 14 (n=34)	St. 15 (n=33)	Surface total (n=116)	Column total (n=668)
$\bar{x}$ pCO_2 µatm	321	326	319	345	329	389
SD µatm	30	60	55	81	63	76
Organic matter Prod./ Remin. (%)	32.9	60.9	57.5	61.7	54.8	83.7
Thermal flux (%)	65.6	33.3	33.1	32.6	35.6	3.4
Water flux (%)	0.2	3.0	3.1	2.7	3.2	0.9
$CaCO_3$ production/dissolution (%)	1.3	2.8	6.3	2.8	6.5	1.9

external ones (stations 13 and 11). In addition, the air–sea CO_2 exchange rate at the inner stations was about an order of magnitude lower than at the external ones. When the studied period was divided according to the four different hydrographic situations mentioned above (IU: intense upwelling; MU: moderate upwelling; R: upwelling relaxation; WC: winter conditions), contrasting behaviours were found even for the same hydrographic situation.

Generally, during intense upwellings high CO_2 water reaches the surface, and a CO_2 flux to the atmosphere is established. In this connection, in winter when photosynthetic activity is low and mixing with subsurface water causes surface pCO_2 to increase influxes of CO_2 to the atmosphere are generally reported. By contrast, a net CO_2 flux into the ocean should be found when high photosynthetic activity is favoured as during moderate upwellings and relaxations of these events.

In more detail, initial pulses of intense upwelling advect CO_2-rich waters to the surface, establishing a net flux to the atmosphere as seen at inner stations in late September 1994 and at stations 13, 14 and 15 in August 1995 (*figure 7*). However, there are some exceptions to this general rule. In July 1994 (intense upwelling period) station 13 was a CO_2 source, whereas station 11 acted as a

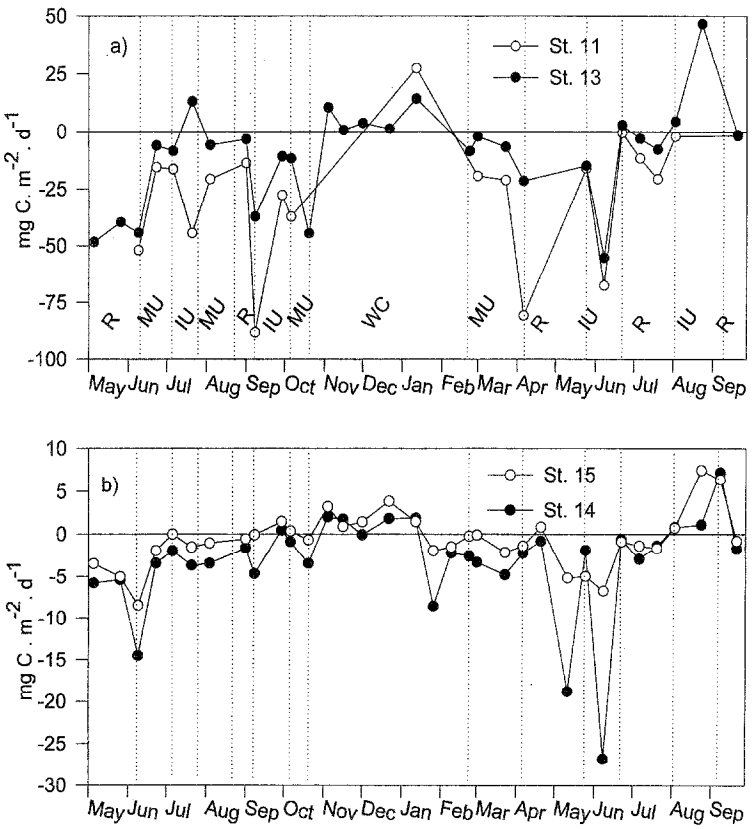

Figure 7. Temporal variability of the air–sea CO_2 flux magnitude (a) at the inner stations and (b) at the offshore stations; the seasonal cycle was grouped according to the hydrographic phases described in the text: IU: intense upwelling, MU: moderated upwelling, WC: winter conditions and UR: upwelling relaxation.

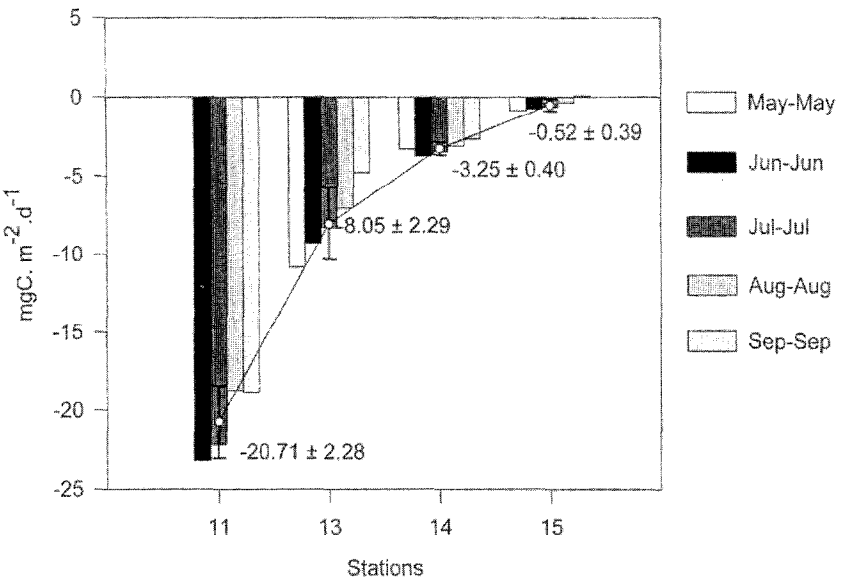

Figure 8. Net CO_2 flux calculated for different annual periods. Mean net fluxes ± standard deviation.

sink because the upwelled water did not reach the surface layer. Moreover, in June 1995, the air–sea CO_2 flux was directed towards the sea, reaching a maximum value of –68 and –55 mg $m^{-2} d^{-1}$ at the external stations and –27 and –5 mg $m^{-2} d^{-1}$ at the inner ones. This fact can be attributed to an enhanced photosynthetic activity in a latter phase of the initial intense upwelling pulse and/or due to coupling of the time scales characteristic of the upwelling process and phytoplankton growth rates.

There were no exceptions to the general behaviour as a CO_2 sink during moderate upwelling and periods of upwelling relaxation, the whole region was a sink for CO_2. Despite this, in winter, fluxes are supposed to be directed towards the atmosphere, as at the inner stations in late October, November and December 1994. However, flux direction reversed in January and February 1995, probably due to an increase in photosynthetic activity as a consequence of higher vertical stability and nutrient availability, both related to a higher runoff [16].

The magnitude of the net annual CO_2 flux will vary depending on the period chosen to perform the calculation given that the seasonal cycle comprised two summers. Thus, *figure 8* shows the net annual CO_2 flux calculated for different time periods together with its mean and standard deviation. The mean net annual CO_2 flux is negative in the four stations, ranging from –0.54 to –22 mg $m^{-2} d^{-1}$, indicating that the Ria of Vigo and adjacent shelf behave as a CO_2 sink on annual time scales.

Average seasonal air–sea fluxes calculated for each station using the CO_2 fluxes in *figure 7* are shown in *table III*. Negative fluxes predominated for most of the seasons and stations. The exception to this generalisation was winter, when fluxes were mainly positive, except in station 14; CO_2 also flowed towards the atmosphere in station 15 during autumn. In summer 1994 higher CO_2 influxes to the ocean were reported than in summer 1995. This fact can be attributed to a higher productivity during summer 1995, as indirectly suggested by surface dissolved oxygen concentrations and upper layer (20 m) integrated chlorophyll *a* averaged over summer 1994 (282 μmol kg^{-1} and 47 mg m^{-2}) and summer 1995 (270 μmol kg^{-1} and 39 mg m^{-2}).

A stepwise, forced to zero, multiple regression was computed in order to ascertain the relative contribution of ΔpCO_2 and k.S on air–sea CO_2 flux on an annual scale. The results of these calculations (*table IV*) indicated that wind speed through piston velocity modulated mainly the CO_2 air–sea exchange on the shelf, whilst inside the Ria, ΔpCO_2 was the principal factor affecting CO_2 exchange.

Table III. Mean seasonal air–sea CO_2 flux (mg $m^{-2} d^{-1}$).

	Sum. 94	Fall	Winter	Spring	Sum. 95
St. 11	–27.1	–51.0	27.4	–34.3	–20.5
St. 13	–9.2	–15.6	2.7	–11.4	–2.0
St. 14	–4.8	–0.8	–1.6	–5.3	–5.0
St. 15	–2.3	0.9	0.5	–2.2	–0.4

4. DISCUSSION

The results presented in this paper clearly indicate that the Ria of Vigo and adjacent shelf waters represent a net

Table IV. Multiple R and percentage of variance explained by pCO_2 gradient (ΔpCO_2) and the exchange coefficient (k.S) on a stepwise, forced to zero, multiple regression between air–sea CO_2 flux and both variables in each station, ($p < 0.001$ in all cases).

Station	Variable	Multiple R	% variance explained
11	ΔpCO_2	0.075	13
	k.S	0.844	71
13	ΔpCO_2	0.751	56
	k.S	0.085	14
14	ΔpCO_2	0.629	40
	k.S	0.110	15
15	ΔpCO_2	0.849	72
	k.S	0.031	6

annual sink for atmospheric CO_2, the magnitude of which varies spatially and temporally.

Few direct quantifications of air–sea CO_2 fluxes on the northwestern Iberian Peninsula have been carried out so far [41]. Previous work indirectly estimated air–sea CO_2 exchange from box models [42], showing that during upwelling periods, when primary production is high, the flux of CO_2 into the ocean can be 127 mg $m^{-2} d^{-1}$, values of the same order as those found in this study in the shelf stations (*figure 7*). The same author calculated a flux to the atmosphere of 85 mg $m^{-2} d^{-1}$ during the downwelling season, a value much higher than the maximum flux estimated for winter conditions for all the sampled stations (25–5 mg $m^{-2} d^{-1}$).

Distinct patterns of CO_2 flux variability were obtained between offshore and inner stations. Station 11 showed the highest mean annual CO_2 flux (*figure 8*) and the lowest coefficient of variation. However, this result should be taken cautiously due to the lack of sampling in those periods when CO_2 is expected to flow towards the atmosphere. At station 11, less influenced by advective processes, subsurface CO_2-enriched seawater did not reach the surface even during intense upwellings and therefore, the direction of the CO_2 flux would be mainly controlled by photosynthetic activity in the upper mixed layer. On the other hand, the decreasing trend of the mean annual CO_2 flux towards the inner part of the Ria is indicative of the strong influence of wind speed on flux magnitude. Thus, variations in this magnitude partly derive from the uncertainty in the parameterization of the gas transfer, as suggested by Lundberg [30] and Wanninkhof [60].

At station 15, the coefficient of the net annual flux variability was 75 %, much higher than that found at the rest of the stations. In this connection, flux direction even slightly reversed when calculated between September 1994 and 1995 (*figure 8*). This fact is related to the higher positive CO_2 fluxes detected in winter and during intense upwelling conditions, and also because the September to September period did not include summer 1994 when air to sea fluxes were maximum. These results are indicative of the importance of selecting an adequate spatial and temporal scale, and reveal the high interannual variability observed in air–sea CO_2 fluxes.

Station 14 stands out as the most intense atmospheric CO_2 sink (mean value –3.4 mg $m^{-2} d^{-1}$) inside the Ria of Vigo. This fact can be attributed to the elevated and negative ΔpCO_2 values generally reported at this station as the CO_2 air–sea exchange at the inner stations was mainly determined by the pCO_2 gradient (*table IV*). ΔpCO_2 was on average three-fold higher at station 14 than at station 15 (*table II*), suggesting that the net photosynthesis-respiration balance was considerably higher at station 14 than at the inner part of the Ria. Enhanced dissolved organic carbon concentrations have been measured in this zone [16]. In addition, the Ria of Vigo supports an intense edible mussel culture which is responsible for the release of great amounts of detrital material to the water [9]. Also, macrophyte populations decay in the inner part of the Ria in autumn. Heterotrophic processes are, therefore, likely to be of higher relevance at the most internal station (station 15), thus reducing the net CO_2 flux.

Annual primary production rates reported for the Rias ranged from 250 gC $m^{-2} yr^{-1}$ [58] to 350 gC $m^{-2} yr^{-1}$ [42], and it has been estimated that about 1 % of the photosynthetically fixed carbon is buried on coastal sediments [65]. Therefore, between 6.9 and 9.6 mgC $m^{-2} d^{-1}$ are thought to be buried in the sediments of the central zone of the Ria. This magnitude is slightly higher but of the same order of the net annual flux of CO_2 from the atmosphere to the Ria (*figure 8*), thus indicating that the studied system is likely to be in stationary state over the temporal and spatial scales evaluated in this investigation.

The statistical method used to quantify the effect of physical and biological variables on pCO_2 has been previously used by different authors [28, 62]. pCO_2 did not correlate with any other variable except dissolved oxygen concentration, pointing to organic matter production and remineralization processes as the main control on pCO_2. On short spatial scales chlorophyll *a* showed a significant correlation with pCO_2 in the North Atlantic [62]. However, in the study presented here, the spatial scale was less than 50 km, the extended temporal period, 18 months, allowed an increasing effect of other factors influencing surface pCO_2 variability, such as advection of

deep, CO_2-rich water, air–sea CO_2 exchange and a potential time lag between grazing of phytoplankton biomass and its subsequent recycling to dissolved inorganic carbon. Surface dissolved oxygen maxima are expected to occur before minimum pCO_2 values as a consequence of the higher rate of O_2 exchange across the surface [13]. In this study, however, oxygen maxima and pCO_2 minima, or vice versa, were coincident, again showing the influence of biological activity on pCO_2 variability. The same conclusion was reached by different authors in diverse areas, such as the southeastern Bering Sea during spring 1980 [13], the North Atlantic [48], and the northern Indian Ocean during pre-monsoon [22].

The conclusions derived from the thermodynamic analysis were completely consistent with the statistical approach. In order of importance, the processes modulating water column and surface pCO_2 variability were organic matter production/remineralisation, thermal and water fluxes and finally, carbonate precipitation/dissolution.

Salinity changes explained between a 0.9 and a 3.2 % of the pCO_2 variability considering the water column and the surface layer, respectively, whereas the calculated value for the global ocean is less than 10 % [54]. This discrepancy could be considered as contradictory because water flux in an estuary is much higher than in the open ocean. However, given the high productivity of these systems [17, 42, 58] the effect of photosynthetic TIC uptake on pCO_2 is expected to be about ten fold that caused by dilution processes. The influence of thermal flux was always much higher than that attributed to dilution processes, especially in the surface layer of station 11. In this regard, we obtained similar values for the $\delta pCO_2/\delta S$ (considering proportional dilution in TIC and Alk.) and $\delta pCO_2/\delta T$ relationships, about 16.5 µatm $°C^{-1}$ or salinity units. Taking into account that surface seasonal thermal changes were wider than salinity variations (coefficients of variation equal to 11 % and 3 %, respectively), the former are expected to affect pCO_2 variability to a larger extent.

In conclusion, the Ria de Vigo and adjacent shelf constitute a net annual atmospheric sink for CO_2, of which the magnitude varies seasonally and spatially, ranging between –0.54 and –22 mg $m^{-2}\,d^{-1}$ for the inner and the outermost parts of the Ria, respectively. pCO_2 variability is primarily controlled by biological activity. The CO_2 air–sea flux in the inner part of the estuary is mainly dominated by the air–sea CO_2 gradient and therefore by biological activity, whereas in the offshore region wind speed through piston velocity exerts a higher control on CO_2 exchange.

Acknowledgements

The authors express their gratitude to the crew of B.O. *Navaz* from the *Instituto Español de Oceanografía*, to R. Penín, M.V. González and G. Casas for their help during sampling at sea, M.V. González, E. Nogueira, R. Penín, M.J. Pazó and T. Rellán who kindly made the data available. They also thank B. Martín for editorial comments, C. Souto for his valuable help and the anonymous reviewers for the suggestions which helped to improve this paper. This work was supported by the *Comisión Interministerial de Ciencia y Tecnología* (CICYT) under project AMB92-0165.

REFERENCES

[1] Álvarez-Salgado X.A., Rosón G., Pérez F.F., Figueiras F.G., Pazos Y., Nitrogen cycling in an estuarine upwelling system, the Ria de Arousa (NW Spain) I, Short-time-scale patterns of hydrodynamic and biogeochemical circulation, Mar. Ecol. Progr. Ser. 135 (1996) 259–273.

[2] Anderson L.A., On the hydrogen and oxygen content of marine phytoplankton, Deep-Sea Res. 42 (1995) 1675–1680.

[3] Andrié C., Oudot C., Genthon C., Merlivat L., CO_2 fluxes in the Tropical Atlantic during FOCAL cruises, J. Geophys. Res. 91 (1986) 11741–11755.

[4] Bakker D.C.E., de Baar H.J.W., Bathmann U.V., Changes of carbon dioxide in surface waters during spring in the Southern Ocean, Deep-Sea Res. II, 44 (1997) 91–127.

[5] Bakun A., Coastal upwelling indices, west coast of North America, NOAA techn. Rep. NMFS-671, 1973, 103.

[6] Bates N.R., Michaels A.F., Knap A.N., Seasonal and interannual variability of oceanic carbon dioxide species at the U.S. JGOFS Bermuda Atlantic Time-series Study (BATS) site, Deep-Sea Res. II, 43 (1996) 347–383.

[7] Brewer P.G., What controls the variability of carbon dioxide in the surface ocean? A plea for complete information, in: Barton J.D., Brewer P.G., Chesselet R. (Eds.), Dynamic processes in the chemistry of the upper ocean, Plenum press, 1986, 246.

[8] Brewer P.G., Wong G.T.F., Bacon M.P., Spencer D.W., An oceanic calcium problem, Earth Plan. Sci. Lett. 26 (1975) 81–87.

[9] Cabanas J. M., González J.J., Mariño J., Pérez A., Roman G., Estudio del mejillón y su epifauna en los cultivos flotantes de la Ria de Arosa III: observaciones previas sobre la retención de partículas y la biodeposición de una batea, Bol. Inst. Españ. Oceanogr. 5 (1979) 44–50.

[10] Castro C.G., Pérez F.F., Álvarez-Salgado X.A., Rosón G., Ríos A.F., Hydrographic conditions associated with the relaxation of an upwelling event off the Galician coast (NW Spain), J. Geoph. Res. 99 (1994) 5135–5147.

[11] Cauwet G., El ciclo del carbono en los océanos, Seminario de Química Marina 5 (1990) 47–58.

[12] Chipman D.W., pCO_2 surface, in: Recueil de donnés par Le Groupe CITHER-2, Vol. 1. (Ed.) Lab. Phys. Oc. (96-01), Brest, France (1996) 167–180.

[13] Codispoti L.A., Friederick G.E., Iverson R.L., Hood D.W., Temporal changes in the inorganic carbon system of the southeastern Bering Sea during Spring 1980, Nature 296 (1982) 296–242.

[14] Dandonneau Y., Sea-surface pressure of carbon dioxide in the eastern equatorial Pacific (August 1991 to October 1992): a multivariate analysis of physical and biological factors, Deep-Sea Res. II, 42 (1995) 349–364.

[15] Dickson A.G., An exact definition of total alkalinity and a procedure for the estimation of alkalinity and inorganic total carbon from titration data, Deep-Sea Res. 28 (1981) 609–623.

[16] Doval M.D., Nogueira E., Pérez F.F., Spatio-temporal variability of the thermohaline and biogeochemical properties and dissolved organic carbon in a coastal embayment affected by upwelling: the Ria de Vigo (NW Spain), J. Mar. Syst. 14 (1998) 135–150.

[17] Fraga F., Fotosíntesis en la Ría de Vigo, Invest. Pesq. 40 (1976) 151–167.

[18] Fraga F., Upwelling off the Galician coast, Northwest Spain, in: Richards F.A. (Ed.), Coast. Upwelling Ser. 1 AGU, Washington, D.C., 1981, 172–182.

[19] Fraga F., Margalef R., Las Rías Gallegas, in: Estudio y Explotación del mar en Galicia (Ed.), Univ. Santiago de Compostela, 1979, pp. 101–121.

[20] Fraga F., Ríos A.F., Pérez F.F., Figueiras F.G., Theoretical limits of oxygen: carbon and oxygen: nitrogen ratios during photosynthesis and mineralisation of organic matter in the sea, Scientia Marina 62 (1998) 161–168.

[21] Gattuso J.P., Picho M., Frankignoulle M., Biological control of air–sea CO_2 fluxes: effect of photosynthetic and calcifying marine organisms and ecosystems, Mar. Ecol. Progr. Ser. 129 (1995) 307–312.

[22] George M.D., Dileep Kumar M., Naqvi S.W.A., Baerjee S., Narvekar P.V., de Sousa S.N., Jayakumar D.A., A study of the carbon dioxide system in the northern Indian Ocean during premonsoon, Mar. Chem. 47 (1994) 243–254.

[23] Kanamori S., Ikegami H., Calcium-alkalinity relationship in the North Pacific, J. Oceanogr. Soc. Japan 38 (1982) 57–62.

[24] Keeling C.D., Whorf T.P., Atmospheric CO_2 records form sites in the SIO air sampling network, in: Trends: A compendium of Data on Global Change, Carbon Dioxide Analysis Center, Oak Ridge National Laboratory, Oak Ridge, Tenn., 1991, USA.

[25] Landrum L.L., Gammon R.H., Feely R.A., Murphy P.P., Kelly K.C., Cosca C.E., Weiss R.F., North Pacific Ocean CO_2 disequilibrium for spring through summer, 1985–1989, J. Geoph. Res. 101 (1996) 28539–28555.

[26] Laws E.A., Photosynthetic quotients, new production and net community production in the open ocean, Deep-Sea Res. I, 38 (1991) 143–167.

[27] Lee K., Millero F.J., Wanninkof R., The carbon dioxide system in the Atlantic Ocean, J. Geoph. Res. 102 (1997) 15693–15707.

[28] Lefèvre N., Andrié C., Dandonneau Y., pCO_2, chemical properties, and estimated new production in the equatorial Pacific in January–March 1991, J. Geophys. Res. 99 (1994) 12639–12654.

[29] Liss P., Merlivat L., Air–sea exchange rates: Introduction and synthesis, in: Buat-Ménard P. (Ed.), The role of Air–sea Exchange in Geochemical Cycling, NATO Adv. Sci. Inst. Ser. 185, Reidel D., Publ. Co., Dordrecht, Holland, 1986, 113–127.

[30] Lundberg L., CO_2 air–sea exchange in the Nordic Seas, An attempt to make an estimate based on data, Oceanol. Acta 17 (2) (1994) 159–175.

[31] Mackenzie F.T., Global Carbon Cycle: some minor sinks for CO_2, in: Flux of Organic Carbon by Rivers and Oceans, US Dep. Energy. Conf. 8009140 (1981) 360–384.

[32] McClain C.R., Chao S.Y., Atkinson L.P., Blanton J.O., De Castillejo F., Wind-driven upwelling in the vicinity of Cape Finisterre, Spain, J. Geophys. Res. 91 (1986) 8470–8486.

[33] Mehrbach C., Culberson C.H., Hawley J.E., Pytkowicz R.M., Measurements of the apparent dissociation constant of carbonic acid in seawater at atmospheric pressure, Limnol. Oceanogr. 18 (1973) 897–907.

[34] Millero F.J., The thermodynamics of the carbon dioxide system in the oceans, Geochim. Cosmochim. Acta 59 (1995) 661–677.

[35] Millero F.J., Byrne R.H., Wanninkhof R., Freely R., Clayton T., Murphy P., Lamb M.F., The internal consistency of CO_2 measurements in the equatorial Pacific, Mar. Chem. 44 (1993) 269–280.

[36] Mouriño C., Fraga F., Fernández F., Hidrografía de la Ria de Vigo 1979–1980, Cuadernos da Área de Ciencias Mariñas, Seminario de Estudos Galegos, 1 (1984) 91–103.

[37] Pérez F.F, Álvarez-Salgado X.A., Rosón G., Ríos A.F., Carbonic-calcium system, nutrients and total organic nitrogen in continental runoff to the Galician Rías Baixas, NW Spain, Oceanol. Acta 15 (1992) 595–602.

[38] Pérez F.F., Fraga F., The pH measurements in seawater on NBS scale, Mar. Chem. 21 (1987a) 315–327.

[39] Pérez F.F., Fraga F., A precise and rapid analytical procedure for alkalinity determination, Mar. Chem. 21 (1987b) 169–182.

[40] Pérez F.F, Ríos A.F., Castro C.G., Rosón G., Mixing analysis of nutrients, oxygen and dissolved inorganic carbon in the

upper and middle North Atlantic Ocean east of the Azores, J. Mar. Syst. 16 (1998) 219–233.

[41] Pérez F.F, Ríos A.F., Rosón G., Sea surface carbon dioxide off the Iberian Peninsula (east North Atlantic Ocean), J. Mar. Syst. 19 (1999) 27–46.

[42] Prego R., General aspects of carbon biogeochemistry in the Ria of Vigo, north-western Spain, Geochim. Cosmochim. Acta 57 (1993) 2041–2052.

[43] Ríos A.F., Fraga F., Pérez F.F., Estimation of coefficients for the calculation of "NO", "PO" and "CO", starting from the elemental composition of natural phytoplankton, Scientia Marina 53 (1989) 779–784.

[44] Ríos A.F., Anderson T.R., Pérez F.F., The carbonic system distribution and fluxes in the NE Atlantic during spring 1991, Progr. Oceanogr. 95 (1995) 295–314.

[45] Ríos A.F., Bingler L.S., Wallace D., Chipman D.W., Álvarez-Salgado X.A., Arlén L., Rosón G., Castro C.G., Johnson K., Carbon dioxide results obtained during the R.V. *Maurice Ewing* cruise in the South Atlantic (WOCE Section A-17), Carbon dioxide Information Acquisition Center (CDIAC), Oak Ridge, TN, in press.

[46] Ríos A.F., Nombela A., Pérez F.F., Rosón G., Fraga F., Calculation of runoff to an estuary, Ria de Vigo, Scientia Marina, 56 (1992) 29–33.

[47] Ríos A.F., Rosón G., Surface pH, alkalinity and pCO_2 measurements, in: Recueil de données par Le Groupe CITHER-2, Vol.3. (Ed.) Lab. Phys. Oc. (97-02), Brest, France, 1996, 64–72.

[48] Robertson J.E., Watson A.J., Langdon C., Ling R.D., Wood J.W., Diurnal variation in surface pCO_2 and O_2 at 60 °N, 20 °W in the North Atlantic, Deep-Sea Res. II, 40 (1993) 409–422.

[49] Rosón G., Pérez F.F., Álvarez-Salgado X.A., Figueiras F.G., Variation of both thermohaline and chemical properties in an estuarine upwelling ecosystem: Ría de Arousa, I, Time evolution, Est. Coast. Shelf Sci. 41 (1995) 195–213.

[50] Roy R.N., Roy L.N., Vogel K.M., Porter-Moore C., Pearson T., Good C.E., Millero F.J., Campbell D.M., The dissociation constants of carbonic acid in seawater at salinities 5 to 45 and temperatures 0 to 45 °C, Mar. Chem. 44 (1993) 249–267.

[51] Sabine C.L. Key R.M., Controls of fCO_2 in the South Pacific, Mar. Chem. 60 (1998) 95–110.

[52] Siegenthaler U., Sarmiento J.L., Atmospheric carbon dioxide and the ocean, Nature 365 (1993) 119–125.

[53] Takahashi T., Broecker W.S., Werner S.R., Brainbridge A., Carbonate chemistry of the surface waters of the worlds oceans, in: Goldberg E.D., Horibe Y., Saruhashi K., (Eds.), Isotope Marine Chemistry, Uchida Rokakuko, Tokyo, 1980, 291–326.

[54] Takahashi T., Olafsson J., Goddard J.G., Chipman D.W., Sutherland S.C., Seasonal variation of CO_2 and nutrients in the high-latitude surface oceans: a comparative study, Glob. Biogeoch. Cycles 7 (1993) 43–878.

[55] Taylor A.H., Watson A.J., Ainsworth M., Robertson J.E., Turner D.R., A modelling investigation of the role of phytoplankton in the balance of carbon at the surface of the North Atlantic, Glob. Biogeoch. Cycles 5 (1991) 151–171.

[56] Taylor A.H., Watson A.J., Robertson J.E., The influence of the spring bloom on carbon dioxide and oxygen concentrations in the surface waters of the northeast Atlantic during 1989, Deep-Sea Res. 39 (1992) 137–152.

[57] UNESCO La escala de salinidades prácticas de 1978 y la ecuación internacional del estado del agua de mar de 1980, Documentos técnicos de la Unesco sobre ciencias del mar 36 (1984) 1–21.

[58] Varela M., Fuentes J.M., Penas E., Cabanas J.M., Producción primaria de las Rías Baizas de Galicia, Cuadernos da Área de Ciencias Mariñas, Seminario de Estudios Galegos 1 (1984) 173–182.

[59] Walsh J.J., How much shelf production reaches the deep sea? in: Berger W.H., Smetacek V.S., Wefer G. (Eds.), Productivity of the ocean: present and past, John Wiley and Sons Ltd. S. Bernhard, Dahlem Konferenzen, 1989, 175–191.

[60] Wanninkhof R., Relationship between wind speed and gas exchange over the ocean, J. Mar. Res. 97 (1992) 7373–7382.

[61] Watson A.J., Robertson J.E. Ling R.D., Air–sea exchange of CO_2 and its relation to primary production, in: Wollast R., Mackenzie F.T., Chou L. (Eds), Interactions of C, N, P and S Biogeochemical Cycles and Global Change, NATO ASI Series, Vol. I 4, Springer-Verlag, 1993, 233–257.

[62] Watson A.J., Robinson C., Robertson J.E., Williams P.J., Fasham M.R., Spatial variability in the sink for atmospheric carbon dioxide in the North Atlantic, Nature 350 (1991) 50–53.

[63] Weiss R.F., Carbon dioxide in water and seawater: the solubility of a non-ideal gas, Mar. Chem. 2 (1974) 203–215.

[64] Weiss R.F., Jahnke R.A., Keeling C.D., Seasonal effects of temperature and salinity on the partial pressure of CO_2 in sea water, Nature 300 (1982) 300–511.

[65] Wollast R., The coastal organic carbon cycle: fluxes, sources, and sinks, in: Mantoura R.F.C., Martin J.-M., Wollast R. (Ed.), Ocean margin processes in Global Change, John Wiley and Sons Ltd., 1991, 365–381.

[66] Wooster W.S., Bakun A., Mclain D.R., The seasonal upwelling cycle along the eastern boundary of the North Atlantic, J. Mar. Res. 34 (1976) 131–141.

[67] Woolf D.K., Thorpe S.A., Bubbles and the air–sea exchange of gases in near-saturation conditions, J. Mar. Res. 49 (1991) 435–466.